Nanoscale

PAPER

View Article Online
View Journal | View Issue

Cite this: *Nanoscale*, 2016, **8**, 17204

Morphology-induced phonon spectra of CdSe/CdS nanoplatelets: core/shell *vs.* core–crown

V. Dzhagan,*[a,b] A. G. Milekhin,[c,d] M. Ya. Valakh,[b] S. Pedetti,[e] M. Tessier,[e] B. Dubertret[e] and D. R. T. Zahn[a]

Received 1st September 2016,
Accepted 13th September 2016

DOI: 10.1039/c6nr06949e

www.rsc.org/nanoscale

Recently developed two-dimensional colloidal semiconductor nanocrystals, or nanoplatelets (NPLs), extend the palette of solution-processable free-standing 2D nanomaterials of high performance. Growing CdSe and CdS parts subsequently in either side-by-side or stacked manner results in core–crown or core/shell structures, respectively. Both kinds of heterogeneous NPLs find efficient applications and represent interesting materials to study the electronic and lattice excitations and interaction between them under strong one-directional confinement. Here, we investigated by Raman and infrared spectroscopy the phonon spectra and electron–phonon coupling in CdSe/CdS core/shell and core–crown NPLs. A number of distinct spectral features of the two NPL morphologies are observed, which are further modified by tuning the laser excitation energy E_{exc} between in- and off-resonant conditions. The general difference is the larger number of phonon modes in core/shell NPLs and their spectral shifts with increasing shell thickness, as well as with E_{exc}. This behaviour is explained by strong mutual influence of the core and shell and formation of combined phonon modes. In the core–crown structure, the CdSe and CdS modes preserve more independent behaviour with only interface modes forming the phonon overtones with phonons of the core.

Introduction

Two-dimensional free-standing semiconductor structures are exciting objects from the fundamental point of view and very promising for applications. They can be handled using transfer processes, such as the Langmuir–Blodgett process or self-assembling,[1] they can be rolled, bent, and adapt their shape to flexible substrates.[2] The free-standing ultrathin semiconductor layers, nanoplatelets (NPLs), can be synthesized by means of colloidal chemistry[3,4] and demonstrate sharp photoluminescence (PL) emission (full width at half maximum, FWHM < 12 nm), polarized ultrafast PL with a high quantum yield,[3–5] anisotropic light absorption,[6] and other very promising properties.[7–13]

Raman spectroscopy has often been employed to study semiconductor nanostructures,[14] including colloidal nanocrystals (NCs).[15–18] In addition to fundamental knowledge about the elementary excitations,[19,20] the phonon spectra provide information on chemical composition,[21–24] strain,[24] and coupling to the environment.[25–27] Raman spectroscopy was applied to study interdiffusion at core/shell interfaces of spherical CdSe/CdS and CdSe/ZnS NCs and nanorods.[17,28–32] The phonon spectra were shown to be very sensitive to the shell thickness and the procedure of its deposition,[28,30] as well as to post-synthesis thermal treatment.[32,33] The detailed knowledge of the phonon spectra of core/shell NCs is also important due to the fact that the phonons of both core and shell materials contribute to the optical properties of NCs.[12,34–39] Moreover, understanding the structure of the core/shell interface for 2D II–VI NCs would facilitate modelling and application of multiple-interface NCs, including also cadmium-free heterosystems like $CuInS_2$/ZnS, for instance.[40] Up to now, the phonons in ultrathin semiconductor layers were studied mainly for epitaxial superlattices (SLs) coherently grown on certain substrates.[41] Those studies were complicated by the effects of substrate induced strain and/or its relaxation *via* dislocations or transition to 3D island growth, as well as contribution of the Raman signal of the substrate.[41,42] Studies of optical phonons of free-standing 2D layers, in contrary, are limited up to now to only the room temperature Raman spectra of colloidal CdSe NPLs of several different thicknesses reported in ref. 43 and surface-enhanced Raman spectroscopy study of single NPLs in ref. 25. Investigations of acoustical vibrations in

[a]*Semiconductor Physics, Technische Universität Chemnitz, D-09107 Chemnitz, Germany. E-mail: volodymyr.dzhagan@physik.tu-chemnitz.de*
[b]*V.E. Lashkaryov Institute of Semiconductor Physics, National Academy of Sciences of Ukraine, 03028 Kyiv, Ukraine*
[c]*A.V. Rzhanov Institute of Semiconductor Physics, 630090 Novosibirsk, Russia*
[d]*Novosibirsk State University, Pirogova street 2, 630090 Novosibirsk, Russia*
[e]*Laboratoire de Physique et d'Étude des Matériaux, PSL Research University, CNRS UMR 8213, Sorbonne Universités UPMC Univ Paris 06, ESPCI ParisTech, 10 rue Vauquelin, 75005 Paris, France*

2D semiconductor nanoparticles were studied before, including the recent work on NPLs by one of the authors.[44] No Raman spectroscopy study of heterogeneous NPLs have been performed up to now. Infrared (IR) spectroscopy was very rarely applied to study phonons in colloidal NCs[45,46] and, to the best of our knowledge, no IR study of any sort of NPLs has been reported yet.

Here we report a Raman and IR study of phonons in heterogeneous CdSe/CdS NPLs of two different designs – core/shell structure and core–crown structure – which show drastic difference regarding the mutual influence of CdSe and CdS parts on the phonon spectra of each other. Raman study was performed at low temperature (35 K) and using various excitation energies (E_{exc}). Complementary IR spectroscopy measurements helped us to conclude about the nature of the phonon modes observed.

Results and discussion

Structural and optical characterization

The synthesis, structural and optical properties of core–crown and core/shell CdSe/CdS NPLs, as well as of plain core CdSe NPLs, studied in this work, were described in detail recently.[4,5] The NPLs of all types are of rectangular shape, with lateral dimensions of tens of nm (Fig. 1), and thicknesses of few nanometers (several monolayers, MLs).[3,4]

The core–crown NPLs were obtained by extending the CdSe NPLs with CdS in the lateral direction (see schematic in the inset to Fig. 2a), while in the case of core/shell NPLs a CdS shell with ML precision was deposited around the CdSe NPL (Fig. 2b, inset).

The UV-vis spectra of bare CdSe NPLs show very sharp absorption features (Fig. 2), which are explained by the absence of NPL thickness variation within the ensemble as well as within each single NPL.[5] In core/shell NPLs the absorption features are broader due to less perfect homogeneity of the shell thickness as compared to that of the core (Fig. 2b).[4] Nevertheless, the first 3–4 electron–hole transitions can be clearly identified in the UV-vis spectra of core/shell NPLs as well. The gradual red shift of the absorption features with increasing shell thickness is a general trend for NCs of core/shell type and is related to the weakening of the electronic confinement due to partial tunneling of the electronic wavefunction into the shell.[4,30] Growing the CdS part as an extension of CdSe (core) in the lateral direction in core–crown NPLs has no effect onto the absorption features related to the CdSe core (Fig. 2a), because the wavefunction in the core is not confined in the lateral direction and thus does not tunnel notably into the shell. This principal difference is reflected in the formation of the phonon spectra of two types of CdSe/CdS NPLs, as will be shown below. In order to facilitate this analysis, we first consider the spectrum of bare CdSe NPLs.

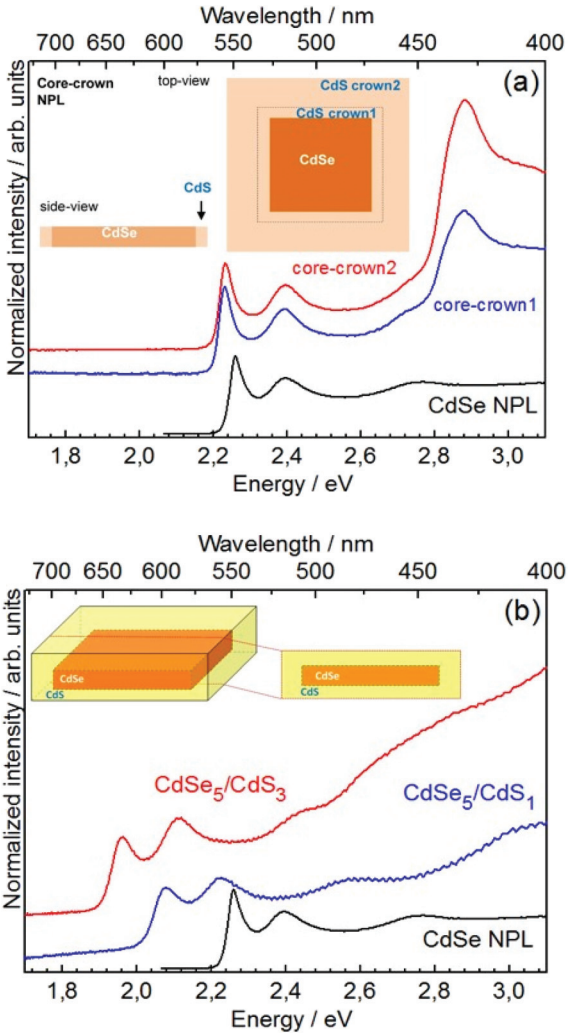

Fig. 2 UV-vis absorption spectra of the (a) core–crown and (b) core/shell NPLs with two different nominal volume of the CdS crown extension and CdS shell thickness, respectively. The sketches of both NPL structures are shown in the insets.

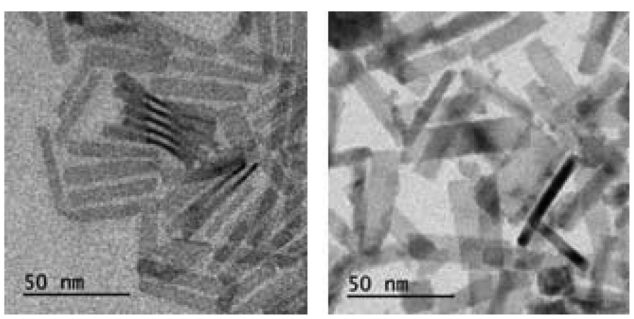

Fig. 1 TEM images of (a) $CdSe_5$ and (b) $CdSe_5/CdS_6$ NPLs.

Raman scattering by phonons in bare CdSe NPLs

The low-temperature resonant Raman spectrum of 5 MLs thick bare CdSe NPLs is presented in Fig. 3 along with its multi-peak fit. The strongest peaks, at 209 cm^{-1}, is due to longitudinal optical (LO) mode, with corresponding second-order (2LO) and third-order (3LO) features occurring at 417 cm^{-1} and

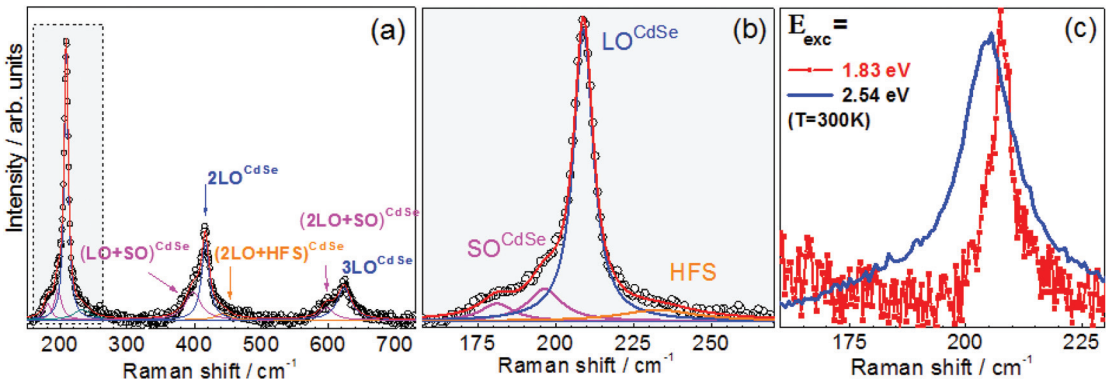

Fig. 3 (a) Resonant Raman spectrum of 5 ML thick CdSe NPLs measured at E_{exc} = 2.7 eV and T = 35 K, along with its multi-peak fit. (b) The 1LO region, shaded in (a), in more detail. (c) The room temperature Raman spectra at resonant (2.54 eV) and non-resonant (1.83 eV) excitation are compared (see text for details).

624 cm^{-1}, respectively.[15,47] The broad weak feature above the LO peaks, denoted in Fig. 3 as HFS (high-frequency shoulder), was previously reported for spherical NCs and presumably assigned either to the surface-induced phonon density of states or to higher-order scattering process involving optical and acoustical vibrations.[48,49]

Recent investigations of CdSe NPLs and spherical NCs by means of surface enhanced Raman scattering additionally suggest a contribution of surface Se to this spectral feature.[27] This could be a plausible assumption for CdSe NCs, because the strongest features of elemental or amorphous Se is known to peak near 250 cm^{-1}.[16] However, an analogous shoulder was reported for CdS and CdTe NCs,[50] but the Raman features of Te are not above but below the LO feature of CdTe,[51] and the elemental sulphur peaks are also far from the CdS LO position.[52]

The lower-frequency shoulder of the LO peak can be fitted with two components (Fig. 3b) and assigned to surface optical (SO) phonons based on previous observations in NCs of other morphologies.[17,18,53] The SO modes are known to occur between the frequencies of TO (transverse optical) and LO phonons of the corresponding bulk material.[17,26,53,54] At T = 35 K ν_{TO}^{CdSe} = 170 cm^{-1} and ν_{LO}^{CdSe} = 213 cm^{-1} and about 3 cm^{-1} lower frequencies are at room temperature.[55] Even though only one SO component was usually reported in the previous studies of spherical NCs and nanorods,[53] a good fit of the NPL spectra requires at least two components in the relevant spectral region. The combination of quasi-zero size distribution of the NPL samples and the low temperature of Raman experiments could be the reason which allowed us to resolve the fine structure of the SO phonon spectra in this work, which was not possible in studies of other NC morphologies which all possess a certain size distribution. We will return to the discussion of the SO modes in the section devoted to core/shell NPLs. Here we only note that the SO modes can be regarded as interface phonons related to the semiconductor/air interface.[41,54] In the range of multi-phonon process, besides 2LO and 3LO scattering, we observe rather strong components matching well combinations of LO and SO modes (Fig. 3a), reported recently also for spherical CdSe NCs.[50] The combination modes will be discussed in more detail also later in this manuscript.

The confinement of the LO phonons in NPLs is expected to occur only in one dimension – along their thickness, because the lateral dimensions are too large to cause phonon confinement. The magnitude of the LO phonon downward shift, $\Delta\nu$, with respect to the bulk ν_{LO}^{CdSe} is about 5 cm^{-1} for our 5 ML CdSe NPLs. However, in the spectra taken at non-resonant excitation, the main phonon peaks occur at higher frequency and have much smaller full width at half maximum (FWHM) compared to those in resonant spectra (Fig. 3c). This result can be explained by probing LO phonons which undergo weaker phonon confinement (*i.e.* smaller $\Delta\nu$) compared to those modes that appear in the resonant spectra. Such an explanation was initially proposed in ref. 43 assuming the confined phonons propagating perpendicular to the NPL plane to dominate in resonant Raman spectra, while those which propagate along the NPL plane and thus non-confined are predominantly observed in non-resonant spectra. In our spectra of 5 ML NPLs (Fig. 2c) we derive the confinement shift of $\Delta\nu$ = 5 cm^{-1} at resonant excitation and 2 cm^{-1} at non-resonant excitation (with respect to the RT bulk CdSe frequency of 210 cm^{-1} (ref. 55)). We may therefore assume that the phonons excited non-resonantly still "feel" confinement, though much weaker than at resonant excitation. A noticeable difference in resonant and non-resonant spectra is also observed for the LO FWHM which is 12 cm^{-1} and 5 cm^{-1}, respectively, corroborating the above assumption about the different degree of phonon confinement. At the same time, from numerous works on semiconductors slabs, thin films, and thin-layer SLs it is known that interface phonon modes can be observed in resonant Raman spectra, while confined LO phonons are the main Raman features at non-resonant excitation.[56] The behaviour of phonon peaks in core/shell NPLs, discussed in a separate section, indicates that the modes observed in Raman spectra at resonant excitation may indeed be not pure LO but partially of interface/surface modes character.

The CdS crown causes a peak near 300 cm^{-1}, which can be assigned to the CdS LO phonon (Fig. 4a and c).[15,55] Its first

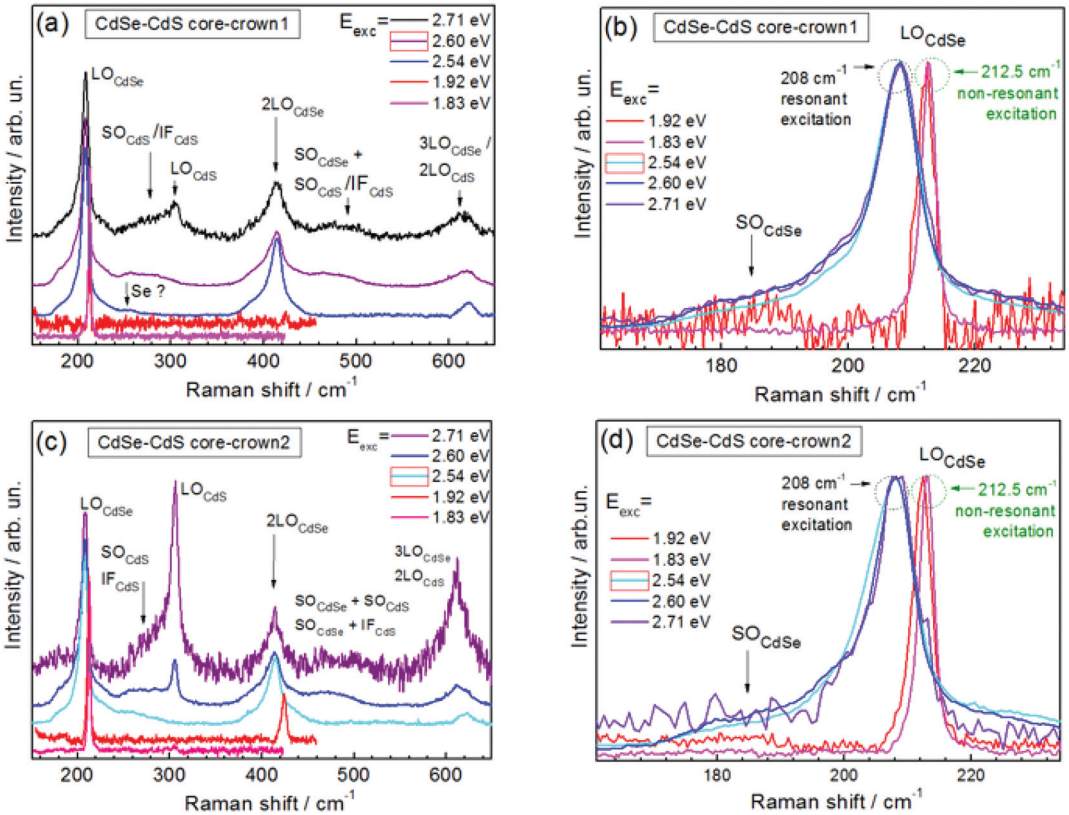

Fig. 4 Raman spectra at resonant (E_{exc} = 2.71, 2.60, 2.54 eV) and non-resonant (E_{exc} = 1.92, 1.83 eV) excitation of CdSe–CdS core–crown NPLs. (b) and (d) show the regions of LO phonons in (a) and (c), respectively.

overtone (2LO), expected near 600 cm^{-1}, is not well pronounced to see without fitting, because it overlaps with the 3LO peak of CdSe. The CdS Raman peaks are detected, however, only at (near-)resonant excitation with the CdS-related absorption band near 2.9 eV in UV-vis spectra (Fig. 2). Such resonant excitation for CdS E_{exc} is 2.60 and 2.71 eV for core–crown2 and 2.71 eV for core–crown1. The excitation of 2.54 eV (and also 2.60 eV in case of core–crown1) causes only broad weak scattering between 240 and 300 cm^{-1}. The feature peaked at 250 cm^{-1} may be related with Se on the surface of CdSe part.[16,27] The broader scattering feature centered near 270 cm^{-1} can be attributed to CdS SO phonon scattering. The latter mode is expected in the frequency range between bulk CdS TO (240 cm^{-1}) and LO (305 cm^{-1})[55] and was repeatedly observed for CdS nanostructures.[15,21,53,57] This feature is also observed for CdSe/CdS core/shell NPLs discussed later in this work. Increasing the nominal volume of CdS crown causes only proportional increase of the CdS phonon peak intensity, which corroborated by the stronger CdS absorption peak at 2.85 eV in UV-vis spectra (Fig. 2a). Growth of CdS crown causes no effect on CdSe peaks or on the feature at 270 cm^{-1} (Fig. 5).

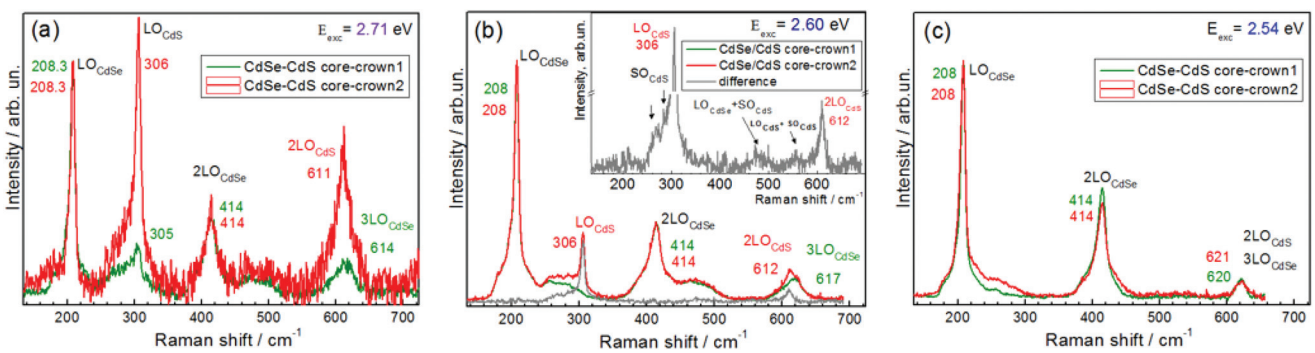

Fig. 5 Overlay of Raman spectra of CdSe-CdS core–crown1 and core–crown2 at different E_{exc}. The grey curve in (b), also shown separately in the inset for clarity, shows the difference between the spectra of the two samples at E_{exc} = 2.60 eV.

Raman scattering by phonons in core–crown NPLs

The spectrum of core–crown NPLs preserves well the main spectral features of the core CdSe NPL (Fig. 4), particularly the position and width of the main phonon peak (LO_{CdSe}) and of its overtones. Besides, the same difference between resonant and non-resonant excitation is observed as in case of bare CdSe NPLs (Fig. 4b and d).

In Raman studies of spherical core/shell NCs the broad scattering feature(s) in the range 260–290 cm^{-1} were proposed to contain (besides CdS SO) the CdS-like mode of the interface alloy.[28,29,33] The distinct difference of the 270 cm^{-1} feature in our crown NPLs as compared to features attributed to alloy modes, is its large FWHM, ~50 cm^{-1}. This value is too large for any "bulk" phonon mode, even in presence of high compositional inhomogeneity and strong spatial confinement of the alloy layer. Besides, the supposed CdS alloy mode must be accompanied by the CdSe counterpart which is expected in the same frequency range as SO_{CdSe}.[15,28] However, corresponding changes in that spectral region are not detected (Fig. 4b and d). Furthermore, with increase of the surface area of the CdS crown from core–crown1 to core–crown2 one could expect both the frequency change and intensity increase of the surface mode, while the interface alloy mode intensity should be saturated after the formation of the interface was finished (*i.e.* should not differ for both core–crown samples studied in this work). Some intensity increase is observed indeed, as can be better seen from the difference spectrum (grey curve at the bottom and in the inset in Fig. 5b) obtained by subtraction of the spectrum of core–crown1 from that of core–crown2. The difference spectrum mimics that of bare CdSe NPLs (with respective account for phonon frequency difference between the CdSe and CdS phonons), except for the weak broad features at around 470 and 550 cm^{-1} (Fig. 5b, inset). Frequency position of these features matches the sum frequencies of LO_{CdSe} + SO_{CdS} or LO_{CdS} + SO_{CdSe} and LO_{CdS} + 270 cm^{-1}, respectively. Increase of this tentative combination mode intensity with increasing the nominal CdS volume and surface area indicates that the coupling between the CdSe and CdS phonon modes in the Raman process is not limited to the near-interface region. Therefore, the broad 270 cm^{-1} mode is more likely dominated by the "external" surface (SO) mode of the CdS crown rather than by the mode related with the interface alloy. Even though CdSe and CdS parts of core–crown NPL possess own/separate resonances in the UV-vis spectra (Fig. 3), leading to pronounced resonances of "own" LO peaks, coupling of the light *via* these resonances to the phonons in the counterpart material/region appears to be quite efficient as well. The enhancement of the interface related broad feature at 250–300 cm^{-1} at (shorter) excitation wavelength favourable for CdS is an expected effect when assuming the latter mode to be SO_{CdS}.

The relative electron phonon coupling strength in CdSe and CdS parts of the core–crown NPL can be estimated from the corresponding 2LO/LO intensity ratio.[19,47] This ratio is not much affected by adding the CdS part in crown (Fig. 4 and 5). This is contrary to the case of core/shell NPLs where the 2LO is notably suppressed by the shell deposition (see next section and Fig. 6), very similar to spherical core/shell NCs reported earlier.[28,30]

Raman scattering by phonons in core/shell NPLs

In contrary to the core–crown structure, growth of CdS in form of core/shell causes tremendous changes in the phonon spectra (Fig. 6). Both CdSe- and CdS modes show several components which change upon increasing shell thickness or E_{exc}. At the resonant excitation (E_{exc} above the absorption onset) spectra of both core–crown NPLs and core/shell NPLs reveal a similar resonant behaviour of the CdS peak intensity, which was observed previously also for spherical core/shell NCs.[28,30] Namely, the relative intensity of the CdS LO features with respect to CdSe ones increases with E_{exc} (Fig. 4–6). However, the spectral changes observed for core/shell NPLs are unique. The splitting of the main LO mode of CdSe core or appearance of new CdSe-related optical modes occurs, which lead to a rich

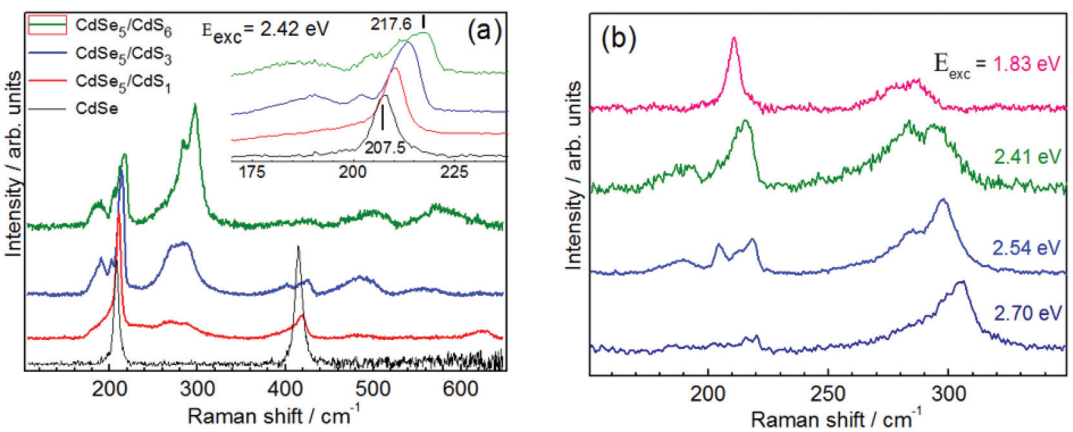

Fig. 6 (a) Raman spectra (E_{exc} = 2.42 eV, T = 35 K) of $CdSe_5/CdS_p$ core/shell NPLs with p = 1,3,6. Inset show the first-order region in more detail. (b) The effect of the E_{exc} on the Raman spectra of $CdSe_5/CdS_{10}$. All the Raman spectra are normalized with respect to the highest peak intensity. The spectra for E_{exc} = 2.41, 2.54, and 2.70 eV were measured at T = 35K, for E_{exc} = 1.83 eV at RT.

spectral pattern in the CdSe spectral region with increase of the CdS shell thickness (Fig. 6a). The enrichment of the CdSe spectral pattern could be explained by the splitting of the intrinsic CdSe LO mode due to shell-induced strain. This may be a plausible explanation for some of the spectral features, particularly for the one which shifts from 207 up to 217 cm^{-1} with shell thickness (Fig. 6a, inset), as the compressive stress in the CdSe core of CdSe/CdS NCs was well determined in Raman spectra as an upward shift of the CdSe LO phonon.[28] However, the position of other spectral features, for instance the CdSe one at ~200 cm^{-1}, is practically not affected by the CdS shell thickness, indicating their nature as being other than "bulk-like" LO. Most probably we deal with the formation of interface(-like) modes in both CdSe and CdS frequency regions. This assumption can be further confirmed by the effect of E_{exc} on the relative intensities and spectral positions of both CdSe and CdS modes. Such a behaviour is not typical for pure LO modes, but it is a characteristic behaviour of interface modes, and it is caused by the selectivity of E_{exc} to certain interface modes according to the matching of the wavevectors of the light and of the phonon.[41,56] The true LO phonon can be the one which remains in the spectrum at off-resonant excitation with 1.83 eV (Fig. 6b). The scattering feature at ~180 cm^{-1} is likely to be an overlap of SO_{CdSe} (or interface phonon) and $CdSe_{alloy}$. Even though this spectral feature undergoes some changes with both shell thickness and E_{exc}, these changes are smaller compared to those of other peaks in both CdSe and CdS regions. Such small changes we would expect for modes related with interface after it was formed. As already discussed above for core–crown NPLs, the broad feature between 450 and 500 cm^{-1} matches well the sum frequencies of the CdSe LO mode at 208 cm^{-1} and of presumably CdS_{SO} band at ~270 cm^{-1} and gets stronger when the latter band gains intensity (Fig. 5b). The same assignment is also applicable to the core/shell NPLs (Fig. 6a). The scattering at 450–500 cm^{-1} spectral range was also observed in our previous works on spherical core/shell NPs.[28,30,50] In those works it was supposed that the spectra contain besides the combination of LO and SO modes also the combination mode of CdSe- and CdS-like modes of the interfacial alloy layer, $CdSe_{alloy}$ + CdS_{alloy}.[28,30] In the case of core–crown NPLs, as discussed above in the text, due to small area of CdSe–CdS interface, as compared to the core/shell NPLs and spherical NCs, as well as due to spectral behaviour discussed in the previous section, the observed coupled CdSe–CdS phonon mode at ~470 cm^{-1} is more likely to be dominated by the mutual combinations of LO and SO modes of CdSe and CdS. Based on the relatively large interface area in core/shell NPLs and the rich spectrum in both CdSe and CdS regions (Fig. 6), we can assume a pair of peaks to be associated with alloying at the interface. Based on Raman studies of spherical NCs and quantum rods,[15,28] the corresponding alloy modes are expected at 200 cm^{-1} ($CdSe_{alloy}$) and 285 cm^{-1} (CdS_{alloy}) and fall in the range of the corresponding SO modes.

Remarkably, different CdSe modes show different 2LO/LO intensity ratio. Particularly, assuming the second-order peaks at 400 and 424 cm^{-1} are corresponding to first-order peaks at 200 and 212 cm^{-1}, respectively, means manifold difference in the 2LO/LO intensity ratio and presumably in the EPC strength. From this fact two alternative conclusions can be drawn: (i) the different LO modes have different coupling strength to the exciton state because of different relative distribution (geometry) of their wavefunctions (the quantum number of the confined optical vibrations can be the relevant characteristic here); (ii) different first order peaks have different nature and thus their coupling to the exciton is different.

IR spectroscopy results

Additional results on the effect of NPL design onto the phonon spectra were obtained from the IR spectra. Due to different selection rules than Raman scattering, the IR spectra are dominated by other types of phonons, particularly by TO and SO ones,[45,46] and are, therefore, complementary to Raman spectra where the most strong features are usually of the LO nature.[25,28,43,47] Representative IR spectra of CdSe, core/shell and core–crown NPLs are shown in Fig. 7.

The detailed IR study of all three types of NPLs will be reported elsewhere, here we only outline some general observations/patterns needed to complete the discussion of the Raman spectroscopy results.

The spectrum of the bare CdSe NPLs is dominated by the band in the range of TO and SO phonons of CdSe (Fig. 7). A notable contribution of normally forbidden LO phonon is also observed, which may corroborate the previously made assumption that the nature of the confined optical vibrations in NCs (vibrons) is of mixed SO–TO–LO character.[58] The spectrum of our core/shell NPLs preserves the features of CdSe and show in addition the strong TO/SO and weak LO features of CdS (Fig. 7).

This observation is fully expected and even the upward shift of the LO_{CdSe} is well explained by the shell induced compres-

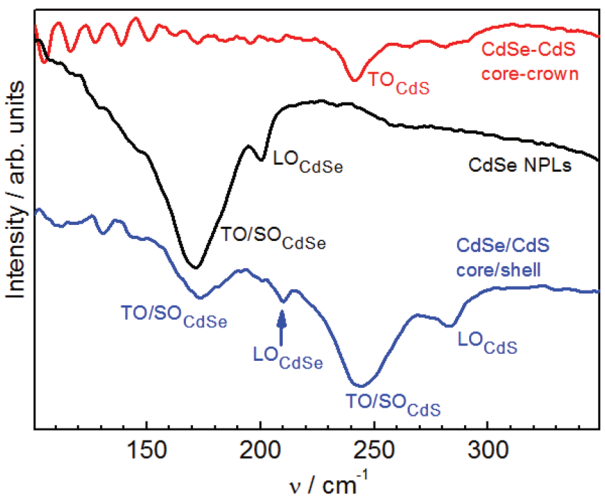

Fig. 7 Representative IR reflectance spectra of CdSe NPLs, CdSe/CdS core/shell and core–crown NPLs.

sive strain and is in complete agreement with the Raman results (Fig. 6a). Differently, the spectrum of CdSe/CdS core–crown NPLs looks rather unexpected. It is dominated by a single relatively sharp feature peaked close to ν_{TO}^{CdS}.[55] Based on the small width of the feature, it is not reasonable to look for notable SO contribution there, and only tiny humps in the range of 250 to 300 cm^{-1} could be interpreted as SO modes (Fig. 7).

Experimental methods

Synthesis of CdSe core, and CdSe/CdS core/shell and core–crown NPLs

For the preparation of CdSe/CdS core/shell NPLs, 2 mL of a solution of 4 MLs CdSe NPLs 3×10^{-6} M in hexane, prepared as described in ref. 3 and 1 mL of *N*-methylformamide (NMF) were charged into a 20 mL vial. Then, 200 μL of a freshly prepared solution of NaSH 0.1 M in NMF were added to the biphasic system and NPLs ligand exchange was observed with a rapid transfer of NPLs to the polar phase. The polar phase containing NPLs was rinsed twice with *n*-hexane and successively precipitated with 2 mL of a toluene : CH_3CN solution in 3 : 1 ratio. The precipitate was dissolved in 0.8 mL of NMF and sonicated for few minutes to allow complete dispersion of the S^{2-} capped NPLs. Here, half a monolayer was grown. The second half monolayer was grown by addition of 120 μL of a solution of $Cd(OAc)_2{\cdot}2H_2O$ at 0.2 M in NMF to the NPLs mixture. After a few minutes of stirring, the NPLs were precipitated with the mixture toluene : CH3CN (3 : 1) and redispersed in 0.8 mL of NMF. After each monolayer the sample was characterized by absorption spectroscopy. The same sequence was repeated as many times as required to grown p layers of CdS shell. Core/shell NPLs were redispersed in a polar solvent performing a ligand exchange with oleic acid and oleylamine. Further in the text we will refer to the core/shell NPLs consisting of n MLs thick CdSe core and p MLs of CdS shell material on each side of the core as $CdSe_n/CdS_p$.

Two CdSe–CdS core–crown NPLs, called further in the text as core–crown1 (small crown) and core–crown2 (large crown), were synthesized as described in ref. 59.

Raman and IR measurements

NPLs were deposited by drop-casting from a solution onto a gold-coated substrate for IR measurements and onto a bare Si substrate for Raman measurements. Non-polarized Raman spectra were excited with the 2.71, 2.60, 2.54, and 2.41 eV lines of an Ar^+ ion laser or the 1.92 or 1.83 eV lines of a Kr^+ ion laser. The spectra were recorded with a Dilor XY triple monochromator equipped with a Peltier cooled CCD detector. The low-temperature measurements were performed at 35 K in a close-cycle helium cryostat (Oxford Instruments). The power of the exciting laser beam was set to 5 mW on the sample surface, after a prior check for laser power dependence of the Raman lineshape. Due to a large laser spot size, ~0.1 mm and cooling of the sample in the cryostat, no measurable heating of the NCs by the laser beam occurred at such laser power. IR reflection spectra were recorded with Fourier transform spectrometer Vertex 80v at room temperature (RT) and light incidence angle of 75°. The resolution was ~2 cm^{-1} in both Raman and IR measurements.

Conclusions

Here, we investigated by Raman and IR spectroscopy the phonon spectra and electron–phonon coupling in CdSe/CdS core/shell and core–crown NPLs. A number of distinct spectral features of the two NPL morphologies are observed, which are further modified by tuning the laser excitation energy E_{exc} between in- and off-resonant conditions. The general trend observed is the larger number of phonon modes in core/shell NPLs and their spectral shifts with increasing shell thickness, as well as with E_{exc}. We can therefore conclude from analysis of the spectra that the layered geometry and thus the large area of CdSe/CdS interface in core/shell NPLs, along with small thickness of core and shell layers, stimulates coupling between the two materials, with formation of additional interface/surface modes and their participation in optical processes like Raman scattering and IR absorption. In the core–crown geometry, in opposite, a more decoupled and bulk-like behaviour of CdSe and CdS dominates (sharp single LO peaks in Raman and TO mode of volume-dominant CdS material in IR). Therefore, even though the complete assignment of the phonon modes we observe in the core–crown and core/shell NPLs has to be done yet, we can already state that heterogeneous NPLs allows for a more powerful shaping the phonon spectrum and also can help understanding the spectra of previously studied spherical NCs.

Acknowledgements

VD, AM, MV and DZ gratefully acknowledge financial support from Volkswagen Foundation, and Alexander von Humboldt Foundation, MERGE project (TU Chemnitz), BD acknowledges support from the ANR, project SNAP. AM is thankful to the Russian Science Foundation (project n.14-12-01037) and the Ministry of Education and Science of the Russian Federation.

Notes and references

1 F. Wang, J.-H. Seo, Z. Ma and X. Wang, *ACS Nano*, 2012, **6**(3), 2602–2609.
2 F. Cavallo and M. G. Lagally, *Soft Matter*, 2010, **6**(3), 439–455.
3 S. Ithurria, M. D. Tessier, B. Mahler, R. P. S. M. Lobo, B. Dubertret and A. L. Efros, *Nat. Mater.*, 2011, **10**(12), 936–941.
4 B. Mahler, B. Nadal, C. Bouet, G. Patriarche and B. Dubertret, *J. Am. Chem. Soc.*, 2012, **134**(45), 18591–18598.

5 S. Ithurria and B. Dubertret, *J. Am. Chem. Soc.*, 2008, **130**(49), 16504–16505.
6 M. V. Mukhina, V. G. Maslov, A. V. Baranov, A. V. Fyodorov, M. V. Artem'ev and A. V. Prudnikov, *J. Opt. Technol.*, 2013, **80**(10), 642.
7 A. Antanovich, A. Prudnikau, A. Matsukovich, A. W. Achtstein and M. Artemyev, *J. Phys. Chem. C*, 2016, **120**, 5764–5775.
8 Q. Li, K. Wu, J. Chen, Z. Chen, J. R. McBride and T. Lian, *ACS Nano*, 2016, **10**, 3843–3851.
9 N. V. Tepliakov, I. O. Ponomareva, M. Y. Leonov, A. V. Baranov, A. V. Fedorov and I. D. Rukhlenko, *J. Phys. Chem. C*, 2016, **120**, 2379–2385.
10 a. Szemjonov, T. Pauporté, S. Ithurria, N. Lequeux, B. Dubertret, I. Ciofini and F. Labat, *RSC Adv.*, 2014, **4**(99), 55980–55989.
11 E. Beaudoin, B. Abecassis, D. Constantin, J. Degrouard and P. Davidson, *Chem. Commun.*, 2015, **51**(19), 4051–4054.
12 A. W. Achtstein, R. Scott, S. Kickhöfel, S. T. Jagsch, S. Christodoulou, G. H. V. Bertrand, A. V. Prudnikau, A. Antanovich, M. Artemyev, I. Moreels, A. Schliwa and U. Woggon, *Phys. Rev. Lett.*, 2016, **116**(11), 116802.
13 I. Moreels, *Nat. Mater.*, 2015, **14**(5), 464–465.
14 S.-L. Zhang, *Raman Spectroscopy and its Application in Nanostructures*, Wiley, 2012.
15 A. G. Rolo and M. I. Vasilevskiy, *J. Raman Spectrosc.*, 2007, **38**(April), 618–633.
16 A. E. Raevskaya, A. L. Stroyuk, S. Y. Kuchmiy, V. M. Dzhagan, D. R. T. T. Zahn and S. Schulze, *Solid State Commun.*, 2008, **145**(5–6), 288–292.
17 A. C. A. Silva, S. W. da Silva, P. C. Morais and N. O. Dantas, *ACS Nano*, 2014, **8**(2), 1913–1922.
18 N. Tschirner, H. Lange, A. Schliwa, A. Biermann, C. Thomsen, K. Lambert, R. Gomes and Z. Hens, *Chem. Mater.*, 2012, **24**(2), 311–318.
19 J. A. Baker, D. F. Kelley and A. M. Kelley, *J. Chem. Phys.*, 2013, **139**(2), 024702.
20 P. Kusch, H. Lange, M. Artemyev and C. Thomsen, *Solid State Commun.*, 2011, **151**(1), 67–70.
21 Y. M. Azhniuk, A. V. Gomonnai, Y. I. Hutych, V. V. Lopushansky, I. I. Turok, V. O. Yukhymchuk and D. R. T. Zahn, *J. Cryst. Growth*, 2010, **312**(10), 1709–1716.
22 V. Izquierdo-Roca, A. Shavel, E. Saucedo, S. Jaime-Ferrer, J. Álvarez-García, A. Cabot, A. Pérez-Rodríguez, V. Bermudez and J. R. Morante, *Sol. Energy Mater. Sol. Cells*, 2011, **95**, S83–S88.
23 E. S. Freitas Neto, S. W. da Silva, P. C. Morais and N. O. Dantas, *J. Phys. Chem. C*, 2013, **117**(1), 657–662.
24 E. S. F. Neto, S. W. da Silva, P. C. Morais, M. I. Vasilevskiy, M. a. Pereira-da-Silva and N. O. Dantas, *J. Raman Spectrosc.*, 2011, **42**(8), 1660–1669.
25 D. O. Sigle, J. T. Hugall, S. Ithurria, B. Dubertret and J. J. Baumberg, *Phys. Rev. Lett.*, 2014, **113**(8), 087402.
26 Y. Wu, S. Jin, Y. Ye, S. Wang, Z. Feng and C. Li, *J. Phys. Chem. C*, 2014, **118**(51), 30269–30273.
27 E. Sheremet, a. G. Milekhin, R. D. Rodriguez, T. Weiss, M. Nesterov, E. E. Rodyakina, O. D. Gordan, L. L. Sveshnikova, T. a. Duda, V. a. Gridchin, V. M. Dzhagan, M. Hietschold and D. R. T. Zahn, *Phys. Chem. Chem. Phys.*, 2015, **17**(33), 21198–21203.
28 V. M. Dzhagan, M. Y. Valakh, A. G. Milekhin, N. A. Yeryukov, D. R. T. T. Zahn, E. Cassette, T. Pons and B. Dubertret, *J. Phys. Chem. C*, 2013, **117**(35), 18225–18233.
29 F. Todescato, A. Minotto, R. Signorini, J. J. Jasieniak and R. Bozio, *ACS Nano*, 2013, **7**(8), 6649–6657.
30 V. M. Dzhagan, M. Y. Valakh, O. E. Raevska, O. L. Stroyuk, S. Y. Kuchmiy and D. R. T. Zahn, *Nanotechnology*, 2009, **20**(36), 365704.
31 S. Christodoulou, F. Rajadell, A. Casu, G. Vaccaro, J. Q. Grim, A. Genovese, L. Manna, J. I. Climente, F. Meinardi, G. Rainò, T. Stöferle, R. F. Mahrt, J. Planelles, S. Brovelli and I. Moreels, *Nat. Commun.*, 2015, **6**, 7905.
32 N. Grumbach, R. K. Capek, E. Tilchin, A. Rubin-Brusilovski, J. Yang, Y. Ein-Eli and E. Lifshitz, *J. Phys. Chem. C*, 2015, **119**, 12749–12756.
33 M. Isarov, N. Grumbach, G. I. Maikov, J. Tilchin, Y. Jang, A. Sashchiuk and E. Lifshitz, *Lith. J. Phys.*, 2015, **55**(4), 297–304.
34 A. W. Achtstein, R. Scott, S. Kickhöfel, S. T. Jagsch, S. Christodoulou, A. V. Prudnikau, A. Antanovich, M. Artemyev, I. Moreels, A. Schliwa and U. Woggon, *Phys. Rev. Lett.*, 2016, **116**, 116802.
35 A. G. del Águila, B. Jha, F. Pietra, E. Groeneveld, C. D. M. Donega, J. C. Maan and P. C. M. Christianen, *ACS Nano*, 2014, **8**(6), 5921–5931.
36 D. Sarkar, H. P. van der Meulen, J. M. Calleja, J. M. Meyer, R. J. Haug and K. Pierz, *Appl. Phys. Lett.*, 2008, **92**(18), 181909.
37 M. J. Fernée, C. Sinito, P. Mulvaney, P. Tamarat and B. Lounis, *Phys. Chem. Chem. Phys.*, 2014, **16**(32), 16957–16961.
38 C. Lin, K. Gong, D. F. Kelley and A. M. Kelley, *ACS Nano*, 2015, **9**(8), 8131–8141.
39 J. Cui, A. P. Beyler, I. Coropceanu, L. Cleary, T. R. Avila, Y. Chen, J. M. Cordero, S. L. Heathcote, D. K. Harris, O. Chen, J. Cao and M. G. Bawendi, *Nano Lett.*, 2015, **16**, 289–296.
40 J. Li, B. Kempken, V. Dzhagan, D. R. T. Zahn, J. Grzelak, S. Mackowski, J. Parisi and J. Kolny-Olesiak, *CrystEngComm*, 2015, **17**, 5634–5643.
41 *Light Scattering in Solids V. Superlattices and Other Microstructures*, ed. M. Cardona and G. Giintherodt, Springer-Verlag, 1989.
42 A. G. Milekhin, A. I. Nikiforov, M. Ladanov, O. P. Pchelyakov, D. a. Tenne, S. Schulze and D. R. T. Zahn, *Phys. Solid State*, 2002, **46**, 92–96.
43 S. A. Cherevkov, A. V. Fedorov, M. V. Artemyev, A. V. Prudnikau and A. V. Baranov, *Phys. Rev. B: Condens. Matter*, 2013, **88**(4), 041303.

44 A. Girard, L. Saviot, S. Pedetti, M. D. Tessier, J. Margueritat, H. Gehan, B. Mahler, B. Dubertret and A. Mermet, *Nanoscale*, 2016, 13251–13256.
45 M. I. Vasilevskiy, A. G. Rolo, M. V. Artemyev, S. A. Filonovich, M. J. M. Gomes and Y. P. Rakovich, *Phys. Status Solidi*, 2001, **224**(2), 599–604.
46 R. B. Vasiliev, V. S. Vinogradov, S. G. Dorofeev, S. P. Kozyrev, I. V. Kucherenko and N. N. Novikova, *Phys. Solid State*, 2007, **49**(3), 547–551.
47 M. C. Klein, F. Hache, D. Ricard and C. Flytzanis, *Phys. Rev. B: Condens. Matter*, 1990, **42**(17), 11123–11132.
48 V. M. Dzhagan, I. Lokteva, M. Y. Valakh, O. E. Raevska, J. Kolny-Olesiak and D. R. T. Zahn, *J. Appl. Phys.*, 2009, **106**(8), 084318.
49 Q. Zhang, J. Zhang, M. I. B. Utama, B. Peng, M. De La Mata, J. Arbiol and Q. Xiong, *Phys. Rev. B: Condens. Matter*, 2012, **85**(8), 085418.
50 V. Dzhagan, M. Valakh, N. Mel'nik, O. Rayevska, I. Lokteva, J. Kolny-Olesiak and D. R. T. Zahn, *Int. J. Spectrosc.*, 2012, **2012**, 532385.
51 P. M. Amirtharaj and F. H. Pollak, *Appl. Phys. Lett.*, 1984, **45**(7), 789–791.
52 V. Toniazzo, C. Mustin, J. M. Portal, B. Humbert, R. Benoit and R. Erre, *Appl. Surf. Sci.*, 1999, **143**(1), 229–237.
53 H. Lange, M. Mohr, M. Artemyev, U. Woggon, T. Niermann and C. Thomsen, *Phys. Status Solidi*, 2010, **247**(10), 2488–2497.
54 R. Fuchs, K. Kliewer and W. Pardee, *Phys. Rev.*, 1966, **150**, 589–596.
55 Landolt-Börnstein - Group III Condensed Matter Volume 44E, 2012.
56 A. K. Sood, J. Menendez, M. Cardona and K. Ploog, *Phys. Rev. Lett.*, 1985, **54**(19), 2115–2118.
57 V. M. Dzhagan, M. Y. Valakh, C. Himcinschi, A. G. Milekhin, D. Solonenko, N. A. Yeryukov, O. E. Raevskaya, O. L. Stroyuk and D. R. T. Zahn, *J. Phys. Chem. C*, 2014, **118**(33), 19492–19497.
58 A. G. Rolo, M. I. Vasilevskiy, M. Hamma and C. Trallero-Giner, *Phys. Rev. B: Condens. Matter*, 2008, **78**(8), 081304.
59 M. D. Tessier, P. Spinicelli, D. Dupont, G. Patriarche, S. Ithurria and B. Dubertret, *Nano Lett.*, 2014, **14**, 207–214.